

## Fullerides of alkaline-earth metals

Y. Chen, F. Stepniak, and J. H. Weaver

*Department of Materials Science and Chemical Engineering, University of Minnesota, Minneapolis, Minnesota 55455*

L. P. F. Chibante and R. E. Smalley

*Rice Quantum Institute and Departments of Chemistry and Physics, Rice University, Houston, Texas 77251*

(Received 25 November 1991)

Synchrotron radiation photoemission studies show that the mixing of Mg, Sr, and Ba with  $C_{60}$  yields metallic (Sr and Ba) and nonmetallic (Mg) fullerides. In all cases, fulleride formation leads to the occupation of hybrid bands near the Fermi level that are derived from  $C_{60}$  states and the  $s$  states of the alkaline-earth atoms. The nonmetallic character of  $Mg_xC_{60}$  probably reflects electron correlation effects, and metallic  $Sr_xC_{60}$  and  $Ba_xC_{60}$  fullerides are candidates for superconductivity.

The reports of conductivity<sup>1</sup> and superconductivity<sup>2</sup> for  $C_{60}$  films exposed to alkali metals stimulated a great deal of research into the properties of the alkali-metal fullerides. It is now clear that the transition to the metallic state is related to the occupation of energy levels derived from the lowest unoccupied molecular orbitals (LUMO) of  $C_{60}$  by electrons donated by the alkali-metal atom.<sup>3,4</sup> The superconducting phase has been identified as  $A_3C_{60}$  for  $A=K$  and Rb, corresponding to complete filling of tetrahedral and octahedral interstitial sites of the  $C_{60}$ -based fcc structure.<sup>5,6</sup> For  $A=Li$  and Na, only semiconducting phases are formed.<sup>7</sup>

To date, reports of fulleride formation have been limited to the alkali metals.<sup>1-8</sup> This paper demonstrates that alkaline-earth deposition onto  $C_{60}$  also produces fullerides. Such mixing was anticipated because the alkaline earths have relatively small cohesive energies (1.51 eV/atom for Mg, 1.72 eV for Sr, 1.90 eV for Ba), small ionization energies (7.64 eV for Mg, 5.69 eV for Sr, 5.21 eV for Ba), and they are found with formal +2 valency in compounds with electronegative elements. Our photoemission valence-band spectra for  $Mg_xC_{60}$ ,  $Sr_xC_{60}$ , and  $Ba_xC_{60}$  show a new band of states 1.1–1.9 eV above the highest occupied molecular orbitals (HOMO) of the  $C_{60}$  host. For  $Sr_xC_{60}$  and  $Ba_xC_{60}$ , the Fermi level ( $E_F$ ) falls within this band and the fullerides are metallic. For  $Mg_xC_{60}$ ,  $E_F$  is pinned at the edge of this band and the fulleride is a semiconductor. It is not known whether the Sr and Ba fullerides are superconductors, but all  $C_{60}$  metallic fullerides found thus far exhibit superconductivity. The nonmetallic character of  $Mg_xC_{60}$  suggests that it joins  $Li_xC_{60}$  and  $Na_xC_{60}$  on the insulating side of a metal-insulator transition mediated by electron correlation.

Phase-pure  $C_{60}$  was obtained by the method described in Ref. 9. The fullerenes were sublimed from Ta boats onto  $n$ -type GaAs(110) surfaces prepared by cleaving in ultrahigh vacuum. The amount of material deposited was determined with a quartz crystal thickness monitor. The  $C_{60}$  films were exposed to a flux of Mg, Sr, or Ba produced by thermal sources. After thorough degassing, deposition could be done at pressures below  $3 \times 10^{-9}$  Torr (the dom-

inant residual gas was  $H_2$  released from the source). The operating pressure was  $\sim 1 \times 10^{-10}$  Torr. The photoemission experiments were done at the Wisconsin Synchrotron Radiation Center using the Minnesota-Argonne monochromator and beam line. Photoemitted electrons were collected with an angle-integrated double-pass cylindrical mirror analyzer. The overall instrumental resolution was  $\sim 0.35$  eV for most of the valence-band spectra discussed here. Core-level results, inverse photoemission results, and STM results will be presented in a longer paper.<sup>10</sup>

Figure 1 shows the photoemission electronic structure for  $Mg_xC_{60}$ . The amount of Mg deposition is noted in angstroms where, for reference, 1-Å Mg corresponds to  $\sim 4.3 \times 10^{14}$  atoms/cm<sup>2</sup> and the surface-layer density of close-packed  $C_{60}$  is  $\sim 1 \times 10^{14}$  molecules/cm<sup>2</sup>. The curve for solid  $C_{60}$  shows spectral features identical to those discussed in Ref. 11. The two leading peaks are derived from  $\pi_p$  orbitals, those between 5 and 10 eV are  $\pi_p$  and  $\sigma_p$  derived, and those beyond 10 eV are  $\sigma_p$  derived.<sup>11</sup> Mg deposition reduces the  $C_{60}$  emission intensity but the rate of decrease indicates Mg- $C_{60}$  mixing rather than Mg accumulation on the surface. Expanded-scale spectra show that  $E_F$  falls at the top of the  $Mg_xC_{60}$  valence band and this also indicates mixing because Mg clustering would yield a metallic cutoff. Conclusive evidence for Mg mixing with  $C_{60}$  was revealed by analysis of Mg  $2p$  core levels.<sup>10</sup> For metallic clusters, the core level is about 1.5 eV lower in binding energy than Mg mixed with  $C_{60}$  and the full width at half maximum is only  $\sim 0.5$  eV as opposed to  $\sim 1.5$  eV for Mg in  $C_{60}$ . We only observed this metallic line shape when the  $C_{60}$  film was saturated with Mg and Mg metal started to form on the surface. Detailed analysis shows that the heights of the two leading HOMO peaks were reduced upon  $Mg_xC_{60}$  formation but their integrated intensities relative to the deeper features were nearly unchanged.

The most significant change in the valence-band spectra for  $Mg_xC_{60}$  is the appearance of emission from a band entirely below  $E_F$ , a band that we attribute to states derived from the LUMO of  $C_{60}$  and the  $s$  states of Mg. Deconvolution shows a feature centered 1.1–1.2 eV above HOMO

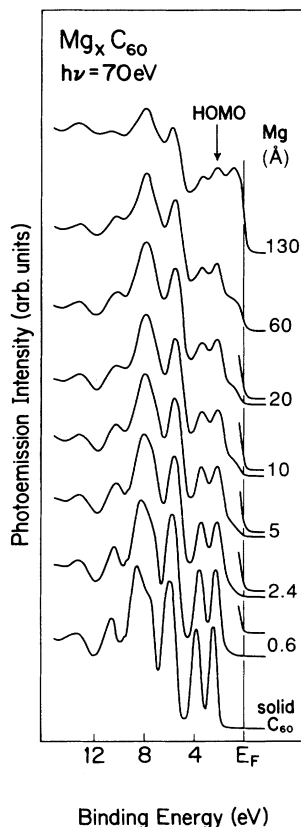


FIG. 1. Valence-band spectra for  $\text{Mg}_x\text{C}_{60}$  growth at 300 K, referenced to the Fermi level. Mg mixing produces line-shape broadening that is particularly evident for the  $\pi_p$  states.  $E_F$  is pinned at the top of the fulleride valence band, a band derived from the LUMO and the alkaline-earth  $s$  states. Metallic character is only evident when Mg clusters form on the surface.

that has a full width at half maximum similar to that of HOMO, i.e., 1.0–1.1 eV. The peak-to-peak energy separation between it and HOMO is close to that for  $\text{Li}_2\text{C}_{60}$  and  $\text{Na}_2\text{C}_{60}$  where another band of states developed below  $E_F$  and semiconducting character was observed.<sup>7</sup> It is considerably smaller than the corresponding separation for  $\text{K}_3\text{C}_{60}$  (1.9 eV) or  $\text{K}_6\text{C}_{60}$  (1.6 eV).<sup>3,4</sup>

The Mg-induced band reflects the nucleation and growth of  $\text{Mg}_x\text{C}_{60}$  phases and it increased with Mg deposition until metallic clusters began to form. By 60-Å coverage, the film had passed the onset of Mg saturation stage and the Mg metal clusters that formed produced a distinct Fermi-level cutoff, as shown. After 130-Å deposition, the photoemission results reflect the superposition of (attenuated) fulleride emission and Mg metal. We can estimate the stoichiometry by using the Mg  $2p$  intensity and assuming that the photoelectron mean free path is 1.4 times greater in  $\text{Mg}_x\text{C}_{60}$  than in Mg metal as suggested by x-ray photoemission results. For  $\sim 15$ -Å Mg deposition, the stoichiometry was then  $x = 3 \pm 1$ . Near the onset of Mg metal cluster formation, which was reached in another growth, the stoichiometry was  $6 \pm 2$ . The error bar is mainly due to uncertainties related to the electron

mean free path in  $\text{Mg}_x\text{C}_{60}$  and, to a lesser extent, the photoionization cross section. This method is not perfect because the intensity reflects the near-surface concentration and it may overestimate the  $x$  value for growth conditions that lead to Mg buildup at the surface, especially when  $x \cong 6$ .

Figure 2 shows valence-band spectra for  $\text{Ba}_x\text{C}_{60}$ . The deposition of 12 Å at 475 K produced a band centered 1.9–2.0 eV above HOMO that was cut by the Fermi level, and there was broadening of the  $\pi_p$ -derived bands. Spectra acquired with higher resolution showed an asymmetric line shape related to the convolution of the Ba-induced structure with the Fermi function. The measured width of the Fermi edge ( $\sim 0.3$  eV, taking the 10%–90% values) approximately reflects the instrument resolution ( $\sim 0.2$  eV) and thermal broadening at 475 K ( $4.4k_B T = 0.18$  eV). The band at  $E_F$  grew with Ba deposition at 475 K, and the HOMO peaks continued to broaden. The LUMO-derived peak was centered 1.8 eV above HOMO by 30-Å deposition. The Ba  $4d$  core-level intensity for this coverage suggests a stoichiometry of  $x = 1 \pm 0.3$ . Further deposition at 475 K resulted in much stronger Fermi-level emission but the intensity was time dependent, demonstrating that the Ba atoms were kinetically trapped near the surface. Since no such limitations were evident during the initial stages of formation, we conclude that the near-surface  $\text{Ba}_x\text{C}_{60}$  phases acted as diffusion barriers (the time needed to relax was  $\sim 40$  min). Higher Ba concentration  $\text{Ba}_x\text{C}_{60}$  was grown at 300 K to avoid the time-dependent behavior observed at 475 K. The disadvantage of low-temperature growth is that the  $\text{Ba}_x\text{C}_{60}$  layer is relatively thin. The highest Ba concentration before metal cluster formation (as judged by Ba  $4d$  core-level

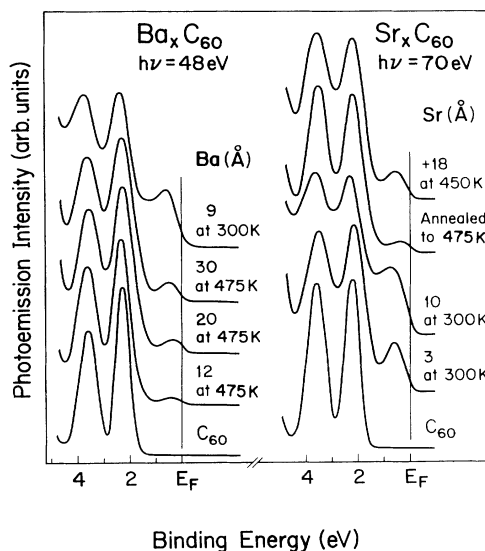


FIG. 2. Valence-band spectra for  $\text{Ba}_x\text{C}_{60}$  and  $\text{Sr}_x\text{C}_{60}$  grown under a variety of conditions. Variations in the intensity of the LUMO- $s$  hybrid band at  $E_F$  reflect surface stoichiometries. Metallic character is evident in all cases. The top left spectrum shows the result of the deposition of 9 Å of Ba on solid  $\text{C}_{60}$  at 300 K.

line shape) was  $x = 6 \pm 2$  and was reached after 9–12-Å Ba deposition. The valence-band spectrum for 9-Å Ba coverage is shown in the top left in Fig. 2.

The right panel of Fig. 2 shows photoemission spectra for Sr deposited on a solid  $C_{60}$  film. Sr deposition of 3 Å at 300 K produced a feature centered  $\sim 1.6$  eV above HOMO. The Sr-induced peak was stronger for 10 Å but it was also broader. The Sr  $3d$  core-level intensities suggest a composition of  $x = 5 \pm 1.5$  at this stage. Annealing to 475 K allowed Sr diffusion into the bulk. The separation between HOMO and the Sr-induced feature also increased to 1.8 eV and the Sr  $3d$  core-level intensity gave a composition of  $x = 0.6 \pm 0.2$ .

The alkaline-earth fullerenes exhibit common characteristics but also fundamental differences. In no case was a transformation out of the metallic stage observed ( $Sr_xC_{60}$  and  $Ba_xC_{60}$  were always metallic,  $Mg_xC_{60}$  was never metallic). Hence, a simple picture in which electrons are transferred to fully occupy the sixfold-degenerate  $t_{1u}$  LUMO levels is not applicable to these fullerenes. For  $K_3C_{60}$ , local-density approximation calculations showed complete charge transfer from the alkali-metal atoms to the LUMO-derived states,<sup>12</sup> consistent with photoemission and inverse photoemission experiments.<sup>3</sup> For alkaline-earth fullerenes, pure ionic bond formation requires the transfer of two  $s$  electrons. This may not be energetically favorable given the rather large second ionization energy for alkaline-earth elements. Therefore, bonding is likely to involve hybridization between  $C_{60}$  states and alkaline-earth states. Note that the two electrons in each alkaline-earth atom will be equally involved in the bonding.

Mixing of the LUMO-derived and the  $s$ -derived states of the alkaline earths is favored because they are close in energy and because the LUMO is unoccupied. In the fullerenes, we do not know if hybridization will result in separation of “bonding” and “antibonding” bands, but we speculate that they will overlap because the respective wave functions are not very localized. Furthermore, LUMO+1 is likely to mix with alkaline-earth  $s$  states, and the bands probably overlap with the LUMO-derived bands. Therefore, it is even less probable that a band gap can exist. For the same reason, a fortuitous band splitting driven by crystal symmetry is not likely to occur over the entire Brillouin zone. The alkaline-earth fullerenes should be metallic since electrons contributed from the alkaline-earth elements can occupy only part of the bands.

Previously, the intensity of the LUMO-derived peak has been used to determine the number of electrons donated by alkali-metal atoms, relating the LUMO and HOMO intensities because they are both  $\pi_p$  derived. For hybrid LUMO- $s$  states, the bond is partially covalent and partially ionic and the stoichiometry cannot be determined reliably with valence-band photoemission. Significantly, the density of states at the Fermi level,  $N(E_F)$ , will be underestimated by such considerations. Although we can conclude that the intensity of the LUMO- $s$  hybrid states increases with doping, we cannot determine  $N(E_F)$ .

Superconductivity in the alkali-metal fullerenes is closely related to distribution of electronic states and those at  $E_F$  are derived almost entirely from the LUMO levels.

Indeed, several studies have focused on electron-electron coupling via  $C_{60}$  phonons although they have not specifically considered the dopant.<sup>12,13</sup> Differences in the superconducting transition temperature for the  $K$ ,  $Rb$ , or  $K_xRb_{1-x}$  fullerenes have been related to  $N(E_F)$ ,<sup>14–16</sup> and every  $C_{60}$  fullerene that exhibits metallic character also shows superconductivity at remarkably high temperature. (The  $Li$  and  $Na$  fullerenes are not metallic in the normal state.<sup>7</sup>)  $Sr_xC_{60}$  and  $Ba_xC_{60}$ , the only metallic fullerenes found outside the alkali-metal family, provide an example of a hybrid conduction band, and we suggest that studies of their low-temperature electrical properties should be interesting.  $Mg_xC_{60}$  stands in sharp contrast because  $E_F$  is pinned at the valence-band maximum. The existence of a gap is confirmed by inverse photoemission and current-voltage measurements using scanning tunneling microscopy.<sup>10</sup>

From the first studies of the electronic states of condensed fullerenes it has been recognized that the fullerenes are narrow-band solids and electron correlation effects are important.<sup>3,7,11,12</sup> Photoemission and inverse photoemission studies of the  $n-1$  and  $n+1$  states have indicated a correlation energy  $U$  of the order of 2 eV. Recently, Gu *et al.*<sup>7</sup> showed the importance of electron-electron correlation for the fullerenes of  $Li_2C_{60}$  and  $Na_2C_{60}$ , compounds that are semiconductors, in contrast to band-structure descriptions. Such behavior was attributed to the localized electronic states and electron-electron repulsion. We propose that the electronic structure of  $Mg_xC_{60}$  also reflects strong electron-electron repulsion, noting that the center-to-center separation between the occupied and unoccupied LUMO- $s$  hybrid bands is  $\sim 2$  eV.<sup>10</sup> This is close to the  $U$  value for the insulating fullerenes.

The atomic and ionic sites of  $Mg$  are much smaller than those for  $Sr$  and  $Ba$ , showing a similar trend when one compares  $Li$  and  $Na$  to  $K$ ,  $Rb$ , and  $Cs$ . It was suggested by Gu *et al.*<sup>7</sup> that the small  $Li$  and  $Na$  ions might not occupy the large octahedral interstitial sites of the fcc  $C_{60}$  lattice. We speculate that the structure of  $Mg_xC_{60}$  would also be different than  $Sr_xC_{60}$  and  $Ba_xC_{60}$ . Such structural changes may not be large enough to split the conduction band in the independent-electron band description, but the system could be pushed to the insulating side of the metal-insulator transition by electron correlation.

In conclusion, we have shown the formation of metallic  $Sr_xC_{60}$  and  $Ba_xC_{60}$  and semiconducting  $Mg_xC_{60}$ . To our knowledge, these are the first fullerenes outside the alkali-metal family. Bonding is through hybridization of the alkaline-earth  $s$  states and the empty states of  $C_{60}$ . The semiconducting nature of  $Mg_xC_{60}$  is attributed to electron correlation. The conducting properties of these solids should be interesting, and synthesis of ternary fullerenes involving alkali-metal and alkaline-earth elements may also be fruitful.

*Note added in proof.* We recently became aware of a paper by Kortan *et al.*<sup>17</sup> confirming that an alkaline-earth fullerene,  $Ca-C_{60}$ , is a superconductor with a transition temperature of  $\sim 8.4$  K.

This work was supported by the Office of Naval Research, the National Science Foundation, and the

Robert A. Welch Foundation. The assistance of the staff at the Wisconsin Synchrotron Radiation Center, a user facility supported by the National Science Foundation, is gratefully acknowledged. Discussions with J. L. Martins, T. R. Ohno, C. Gu, D. M. Poirier, M. B. Jost, and P. J. Benning have been very stimulating.

- 
- <sup>1</sup>R. C. Haddon *et al.*, *Nature (London)* **350**, 320 (1991).  
<sup>2</sup>A. F. Hebard *et al.*, *Nature (London)* **350**, 600 (1991).  
<sup>3</sup>P. J. Benning, J. L. Martins, J. H. Weaver, L. P. F. Chibante, and R. E. Smalley, *Science* **252**, 1417 (1991); P. J. Benning, D. M. Poirier, T. R. Ohno, Y. Chen, M. B. Jost, F. Stepniak, G. H. Kroll, J. H. Weaver, J. Fure, and R. E. Smalley, *Phys. Rev. B* **45**, 6899 (1992).  
<sup>4</sup>G. K. Wertheim, J. E. Rowe, D. N. E. Buchanan, E. E. Chaban, A. F. Hebard, A. R. Kortan, A. V. Makhija, and R. C. Haddon, *Science* **252**, 1419 (1991); C. T. Chen *et al.*, *Nature (London)* **352**, 603 (1991).  
<sup>5</sup>O. Zhou, J. E. Fischer, N. Coustel, S. Kycia, Q. Zhu, A. R. McGhie, W. J. Romanow, J. P. McCauley, A. B. Smith, and D. E. Cox, *Nature (London)* **351**, 462 (1991).  
<sup>6</sup>P. W. Stephens, L. Mihaly, P. L. Lee, R. L. Whetten, S.-M. Huang, R. B. Kaner, F. Diederich, and K. Holzer, *Nature (London)* **351**, 632 (1991).  
<sup>7</sup>C. Gu, F. Stepniak, D. M. Poirier, M. B. Jost, P. J. Benning, Y. Chen, T. R. Ohno, J. L. Martins, J. H. Weaver, L. P. F. Chibante, and R. E. Smalley, *Phys. Rev. B* **45**, 6348 (1992).  
<sup>8</sup>S. P. Kelty, C. Chen, and C. M. Lieber, *Nature (London)* **352**, 223 (1991).  
<sup>9</sup>R. E. Haufler *et al.*, *J. Phys. Chem.* **94**, 8634 (1990); R. E. Haufler, Y. Chai, L. P. F. Chibante, J. Conceicao, C. Jin, L.-S. Wang, S. Maruyama, and R. E. Smalley, *Mater. Res. Soc. Symp. Proc.* **206**, 627 (1991).  
<sup>10</sup>M. B. Jost, Y. Chen, F. Stepniak, Y. Z. Li, J. H. Weaver, and R. E. Smalley (unpublished).  
<sup>11</sup>J. H. Weaver, J. L. Martins, T. Komeda, Y. Chen, T. R. Ohno, G. H. Kroll, N. Troullier, R. E. Haufler, and R. E. Smalley, *Phys. Rev. Lett.* **66**, 1741 (1991).  
<sup>12</sup>J. L. Martins, N. Troullier, and M. Schabel (unpublished).  
<sup>13</sup>M. Schluter, M. Lannoo, M. Needels, G. A. Baraff, and D. Tomanek, *Phys. Rev. Lett.* **68**, 526 (1992); M. Schluter (private communication).  
<sup>14</sup>R. M. Fleming, A. P. Ramirez, M. J. Rosseinsky, D. W. Murphy, R. C. Haddon, S. M. Zahurak, and A. V. Makhija, *Nature (London)* **352**, 787 (1991).  
<sup>15</sup>G. Sparn, J. D. Thompson, S.-M. Huang, R. B. Kaner, F. Diederich, R. L. Whetten, G. Gruner, and K. Holzer, *Science* **252**, 1829 (1991).  
<sup>16</sup>O. Zhou, G. B. M. Vaughan, Q. Zhu, J. E. Fischer, P. A. Heiney, N. Coustel, J. P. McCauley, Jr., and A. B. Smith III, *Science* **255**, 833 (1992).  
<sup>17</sup>A. R. Kortan *et al.*, *Nature (London)* **355**, 529 (1992).